

## Stereochemical Sensitivity of the Human UDP-glucuronosyltransferases 2B7 and 2B17

Ingo Bichlmaier,<sup>†</sup> Antti Siiskonen,<sup>†</sup> Moshe Finel,<sup>‡</sup> and Jari Yli-Kauhaluoma<sup>\*,†</sup>

Faculty of Pharmacy, Division of Pharmaceutical Chemistry, University of Helsinki, FI-00014 Helsinki, Finland, and  
Faculty of Pharmacy, Drug Discovery and Development Technology Center, University of Helsinki, FI-00014 Helsinki, Finland

Received November 14, 2005

A set of 28 enantiomers comprising rigid and flexible secondary alcohols was synthesized by the asymmetric Corey–Bakshi–Shibata reduction. The enantiomerically pure alcohols were subjected to enzymatic glucuronidation assays employing the human UDP-glucuronosyltransferases (UGTs) 2B7 and 2B17. Both UGTs displayed high levels of stereoselectivity, favoring the conjugation of the (*R*)-enantiomers over their respective (*S*)-stereoisomers at eudismic ratios up to 256. The spatial arrangement of the hydroxy group determined the diastereoselectivity of the UGT2B17-catalyzed reaction in agreement with Pfeiffer's rule (eudismic activity quotient =  $0.83 \pm 0.14$ ). Inhibition studies revealed that the enantiomers had similar affinities toward the enzymes. The diastereoselectivity of the UGT-catalyzed conjugation stemmed, therefore, from the arrangement of the substrates in the catalytic site, rather than from distinct affinities toward the enzymes. Taken together, this study showed that metabolic enzymes that are generally conceived to be rather "flexible" in nature are capable of displaying high levels of chiral distinction.

### Introduction

It has long been known that the stereochemistry of chiral xenobiotics determines their pharmacodynamic, pharmacokinetic, and toxicological profiles.<sup>1</sup> These differences in pharmacological and toxicological action are based on the distinct interactions between chiral entities and the homochiral functional constituents of the human body such as receptors, enzymes, and transport proteins.<sup>2,3</sup> In recent years, the advent of efficient asymmetric synthesis enabling the production of single-enantiomer entities at high optical purities, together with progresses in developing efficient purification and analytical methods for these chiral compounds, has paved the way for investigations on the stereoselective outcomes of chiral interactions in the organism.<sup>4</sup> In drug design and development, these advances resulted in the development of optically pure drugs by neglecting the nonactive, less active, or even toxic stereoisomeric "ballast".<sup>5</sup> Detailed insights into stereoselective pharmacological events have led to the understanding that single-enantiomer drugs are often superior over the administration of isomeric mixtures and, therefore, new chiral drugs are approved today virtually exclusively as enantiopure entities.<sup>6–8</sup> It is therefore important to identify biochemical pathways in the human organism susceptible to stereoselective events such as the metabolism by UDP-glucuronosyltransferases (UGTs,<sup>a</sup> EC 2.4.1.17), involved in the deactivation, activation, and toxication of achiral and chiral compounds.<sup>9–11</sup>

UGTs are important enzymes of the human phase-II metabolic system. These enzymes are functionally characterized by the

transfer of the hydrophilic  $\alpha$ -D-glucuronic acid (GlcA) from UDP-glucuronic acid (UDPGlcA) to lipophilic substrates bearing hydroxy, thiol, amino, carboxy groups, and even enolate moieties.<sup>12</sup> This conjugation reaction increases the water solubility of the aglycones and aids in their excretion to prevent the accumulation of endobiotics and xenobiotics to undesirable, or even toxic, levels. Prominent chiral endobiotics and xenobiotics that are glucuronidated by UGTs include the opioid analgesic morphine, the nonsteroidal anti-inflammatory drugs ibuprofen and ketoprofen, the steroids testosterone, estriol, and ethinylestradiol, and the anxiolytic oxazepam as well as the terpenoid alcohols menthol and thymol.<sup>13</sup>

The mechanism of the UGT-catalyzed glucuronidation is essentially unknown, and the crystal structure of these membrane-bound proteins has not yet been resolved. The transition from reactants to products proceeds with inversion of configuration at the anomeric carbon atom of GlcA, and it is therefore assumed that the transfer step is concerted and resembles the bimolecular nucleophilic substitution reaction ( $S_N2$ ). In addition, it is presumed that the cosubstrate binding site resides in the carboxy-terminal half of the protein, which represents a highly conserved region among different UGT isoforms.<sup>14–16</sup> The substrate binding site is presumably located in the amino terminus of the enzymes. Recently, it was shown that UGT1A isoforms display a compulsory ordered mechanism in which UDPGlcA is the first-binding substrate.<sup>17</sup>

UGTs, like other metabolic enzymes, are multifunctional and accept substrates with a wide range of different chemical structures. In the case of UGTs, this is also referred to as promiscuity, or loose fit, and these enzymes are, therefore, commonly described to possess a high degree of "flexibility" to depict their complex and partly overlapping substrate specificities.<sup>18</sup> This could be the reason metabolic enzymes are generally not subjected to eudismic analysis using whole series of chiral compounds.<sup>2</sup> However, this study showed that also these "flexible" UGTs can display great stereochemical selectivity similar to highly specialized receptor proteins. It should be noted here that the complex substrate selectivity of the UGT-catalyzed glucuronidation has been often addressed in the literature, and studies employing computational chem-

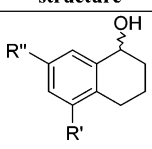
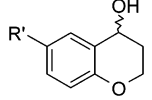
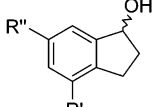
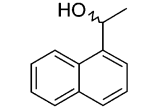
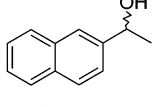
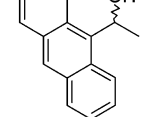
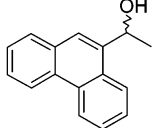
\* Corresponding author. Address: Faculty of Pharmacy, Division of Pharmaceutical Chemistry, P.O. Box 56, University of Helsinki, FI-00014 Helsinki, Finland. Phone: +358 9 19159170. Fax: +358 9 19159556. E-mail: jari.yli-kauhaluoma@helsinki.fi.

<sup>†</sup> Division of Pharmaceutical Chemistry.

<sup>‡</sup> Drug Discovery and Development Technology Center.

<sup>a</sup> Abbreviations: AIC<sub>C</sub>, corrected Akaike's information criterion; CI<sub>95%</sub>, 95% confidence interval; EA, eudismic analysis; EAQ, eudismic activity quotient; EI, eudismic index; ER, eudismic ratio; GlcA, glucuronic acid; IC<sub>50</sub>, concentration of inhibitor which causes 50% inhibition; K<sub>ic</sub>, competitive inhibition constant; K<sub>in</sub>, uncompetitive inhibition constant; R<sup>2</sup>, goodness of fit; K<sub>m</sub>, Michaelis–Menten constant; SAR, structure–activity relationship; SD, standard deviation; UDPGlcA, UDP-glucuronic acid; UGT, UDP-glucuronosyltransferase; V<sub>max</sub>, maximum velocity; v<sub>R</sub>, rate of (*R*)-enantiomer conjugation; v<sub>S</sub>, rate of (*S*)-enantiomer conjugation.

**Table 1.** The Structures of the Enantiomerically Pure Secondary Alcohols Employed in This Study<sup>a</sup>

structure	entry	R'	R''
	1	H	H
	2	CH <sub>3</sub> O	H
	3	H	CH <sub>3</sub> O
	4	H	NO <sub>2</sub>
	5	CH <sub>3</sub>	CH <sub>3</sub>
	6	H	
	7	CH <sub>3</sub>	
	8	H	H
	9	CH <sub>3</sub>	H
	10	H	CH <sub>3</sub>
	11		
	12		
	13		
	14		

<sup>a</sup> The rigid enantiomers include the entries 1–10, and the flexible stereoisomers comprise the entries 11–14.

istry tools led to predictive models for some UGT1A isoforms.<sup>19,20</sup>

In this study we investigated the stereoselective events during the formation of the enzyme–substrate complex and the GlcA-transfer reaction, employing a large set of enantiopure compounds comprising both rigid cyclic and flexible aliphatic alcohols (Table 1). The enantiomers possess only one element of chirality, i.e., the asymmetric carbon atom bearing the nucleophilic hydroxy group, the very site of the UGT-catalyzed glucuronidation. Therefore, the only difference between the enantiomers of each compound is in the spatial arrangement of this nucleophilic group, whereas the physicochemical properties remain per definitionem identical in an achiral environment. By including both flexible and rigid secondary alcohols, we could address the question whether the freely rotating hydroxy group of the flexible alcohols was able to overcome stereoselective events that were observed for rigid alcohols during UGT-catalyzed glucuronidation. The rigid stereoisomers comprise the bicyclic alcohols 1–10 (Table 1), in which the spatial flexibility of the hydroxy group is impaired and, therefore, its position in space is rather well-defined. This is due to the partially unsaturated bicyclic structure hindering the rotation along the  $\sigma$ -bonds in the vicinity of the hydroxy group. In the case of the flexible alcohols, however, the hydroxy group rotates freely because the aliphatic nature of the secondary alcohols does not impair the rotation along the  $\sigma$ -bonds (Table 1, entries 11–14). The UGTs 2B7 and 2B17 were chosen because these enzymes play an important role in the glucuronidation of chiral

entities such as steroids, oxazepam, and profen as well as opioid analgesics.<sup>13,21–23</sup> In addition, we showed previously by conducting screening assays that both enzymes glucuronidated the enantiomers of 1-tetralol, 1-indalol, and 1-benzosuberol.<sup>24</sup>

By employing the enantiomerically pure enantiomers to measure their affinities to the UGTs 2B7 and 2B17 and their rates of UGT-catalyzed conjugation, the influence of the spatial orientation of the hydroxy group and of the substitution pattern on these processes could be directly studied. Eudismic analysis (EA), in general, provides a valuable approach to elucidate the interaction between chiral compounds and their target proteins.<sup>25,26</sup> In addition, this analytical method is used in drug design and development to increase the selectivity and potency of chiral lead compounds toward their receptors.<sup>27</sup> In this study, the tools of EA were employed to identify the factors determining affinity and GlcA-transfer to edge closer to the mechanism of the UGT-catalyzed glucuronidation reaction at the molecular level.

## Results and Discussion

The enantiomers were synthesized by the asymmetric reduction developed by Corey et al.<sup>28,29</sup> The Corey–Bakshi–Shibata (CBS) catalyst was prepared in situ by the addition of trimethyl borate to a solution of (*R*)- or (*S*)-1,1-diphenylprolinol in toluene.<sup>30,31</sup> The addition of a borane *N,N*-diethylaniline complex serving as the reducing agent, followed by the prochiral ketone, afforded the enantiomeric alcohols in excellent yields and high optical purities (cf. Supporting Information).<sup>32</sup> Subsequently, the synthesized substrates were recrystallized several times until an enantiomeric excess of >99.9% for each enantiomer was reached because it was previously shown that eudismic analysis depends strongly on the optical purity of the stereoisomers.<sup>33</sup> In the case of liquid products, the enantiomers were resolved by high-performance liquid chromatography (HPLC) with the use of a chiral (*R,R*)-ULMO column.

The first part of this study is concerned with the differences between the synthesized enantiomerically pure alcohols with respect to the rate of the UGT-catalyzed GlcA-transfer reaction. Therefore, the diastereoselectivity, or substrate–product stereoselectivity,<sup>34</sup> of the enzymatic glucuronidation was studied by comparing the rates of (*R*)- and (*S*)-enantiomer conjugation. In this respect, the velocity of the conjugation reaction catalyzed by UGT2B7 and UGT2B17 for each enantiomer was measured. The concentrations of formed glucuronide for the bicyclic alcohols 1–10 were, however, not sufficient for UV detection, and therefore, the enzyme assays were conducted employing radiolabeled [<sup>14</sup>C]UDPGlcA in combination with “cold” UDPGlcA at a final concentration of 120  $\mu$ M.<sup>35</sup> This procedure had the advantages that the formed [<sup>14</sup>C] $\beta$ -D-glucuronides were readily detected and unambiguously identified and that the amount of product could be directly quantified.<sup>36</sup>

The reaction rates were determined by recording progression curves (Figure 1). This analytical method ensured the comparability and consistency of the data because nonlinear kinetic behavior within the time frame of the enzyme assays was readily detected and subsequently omitted from regression analysis. It should be noted here that as a rule of thumb the formed [<sup>14</sup>C]-glucuronides of (*R*)-enantiomers were readily detected at incubation times between 10 and 60 min and the [<sup>14</sup>C]GlcA-conjugates of (*S*)-enantiomers between 70 and 120 min of incubation (Figure 1). The bicyclic alcohols 1–10 were assayed at a saturating concentration of 2.0 mM, yielding a good estimate of the  $V_{\max}$  under the assay conditions (Figure 1). The flexible alcohols 11–14, however, were employed at unsaturating

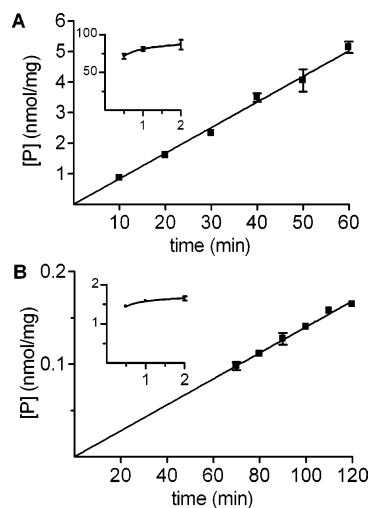


**Figure 1.** Progression curves for the UGT2B17-catalyzed glucuronidation of (*R*)-2 (A) and (*S*)-2 (B). Both enantiomers were assayed at a saturating concentration of 2.0 mM as can be seen from the insets (ordinate, velocity in  $\text{pmol min}^{-1} \text{mg}^{-1}$ ; abscissa, substrate concentration in mM). The enzyme was employed at  $1.0 \mu\text{g}/\mu\text{L}$ , and the UDPGlcA concentration was  $120 \mu\text{M}$ . The slope (velocity) was determined by linear regression (the intercept was constrained to zero). The rate for the (*R*)-2 conjugation was determined to be  $84 \text{ pmol min}^{-1} \text{mg}^{-1}$ , the velocity for the (*S*)-2 glucuronidation was  $1.4 \text{ pmol min}^{-1} \text{mg}^{-1}$ . The detection limit for the (*S*)-2 glucuronide was  $\sim 125 \text{ nM}$ , corresponding to  $\sim 10 \text{ pmol}$  glucuronide ( $80 \mu\text{L}$  injection). The signal-to-noise ratio for the smallest [ $^{14}\text{C}$ ]glucuronide peak was 5.7. The ordinate displays the amount of product formed per milligram of protein. The mean values and the standard deviation ( $n = 2$ ) are shown.

concentrations of 0.10 mM because of their low solubility, and therefore, their measured rates did not resemble their  $V_{\text{max}}$  values.

The results of the rate measurements are displayed in Figure 2, and both enzymes were found to display high degrees of diastereoselectivity during the UGT-catalyzed GlcA-transfer reaction toward the employed enantiomeric alcohols. In this respect, the UGTs 2B7 and 2B17 strongly favored the glucuronidation of the (*R*)-enantiomers over their respective (*S*)-stereoisomers. The sole exception was the flexible alcohol **11** because its enantiomers (*R*)-**11** and (*S*)-**11** were glucuronidated by UGT2B7 at comparable rates of approximately  $30 \text{ pmol min}^{-1} \text{mg}^{-1}$  (Figure 2). It can also be seen that UGT2B17 displayed higher levels of stereoselectivity than UGT2B7. This finding was quantified by calculating the eudismic ratios (ER) for each pair of enantiomers, and the results of this analysis are shown in Table 2. The ER is a useful indicator for the stereoselectivity of biochemical processes. It is calculated by dividing the velocity of the more active enantiomer (eutomer) by the rate of the corresponding less active stereoisomer (distomer). The higher this ratio, the more pronounced the stereoselectivity, or chiral distinction,<sup>37</sup> during the process under investigation. The ERs for UGT2B7 ranged between 1.10 and 58.1, and for 10 out of the 13 compounds the ERs were below 10.0. In contrast, UGT2B17 favored the (*R*)-enantiomers over their corresponding (*S*)-stereoisomer by factors ranging from 8.22 to 256, and only 1 out of the 13 values was found to be below 10.0 (Table 2). Notably, the highest ERs were measured for the UGT2B17-catalyzed conjugation of compounds **5**, **7**, and **10** (ER > 100). Alcohol **5** displayed the highest degree of stereoselectivity, as indicated by its ER of 256.

The only difference between the enantiomers of each compound was in the spatial arrangement of the nucleophilic hydroxy group. Therefore, the underlying principle for the

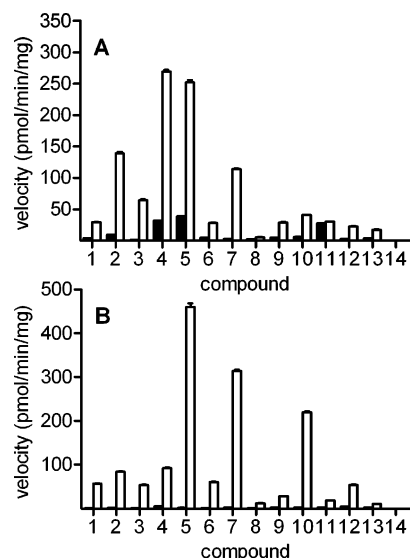


**Figure 2.** The velocities of the UGT-catalyzed glucuronidation for the enantiomeric alcohols **1–14** as determined from the slope of the respective progression curves (the error bars represent the respective standard deviations,  $n = 12$ ). Panel A displays the conjugation rates for the glucuronidation catalyzed by UGT2B7, and panel B shows the glucuronidation velocities for the UGT2B17-catalyzed conjugation. The white and black bars represent the velocities for (*R*)- and (*S*)-enantiomers, respectively. Both enzymes displayed high levels of stereoselectivity with respect to the GlcA-transfer reaction, strongly favoring the glucuronidation of the (*R*)-enantiomers over their respective (*S*)-enantiomers (with the only exception of compound **11** in panel A). The enantiomers of compound **14** were not found to be glucuronidated either by UGT2B7 or by UGT2B17.

diastereoselective GlcA-transfer is the spatial orientation of this group. However, when the ERs of the compounds were compared, it became clear that the substituents exerted a significant influence on the stereoselectivity of this process. This can be readily seen by comparing the ERs of the 4-chromanol derivatives **6** and **7** glucuronidated by UGT2B17 (Table 2). The ER for compound **6** was 50.2, whereas its methylated derivative **7** displayed a 2.6-fold increased stereoselectivity (ER = 131), and the reason for this shift toward higher stereoselectivities could be ascribed to the introduction of the methyl group to the 4-chromanol scaffold of compound **6** as subsequently described. The enantiomer (*S*)-**6** was glucuronidated at a rate of  $1.2 \text{ pmol min}^{-1} \text{mg}^{-1}$ , and its methylated derivative (*S*)-**7** was glucuronidated at a rate of  $2.4 \text{ pmol min}^{-1} \text{mg}^{-1}$  (Table 2). Therefore, the methylation of (*S*)-**6** affording (*S*)-**7** induced a 2-fold increase in the glucuronidation rate. In contrast, the enantiomer (*R*)-**6** was conjugated by UGT2B17 at  $60.8 \text{ pmol min}^{-1} \text{mg}^{-1}$ , and its derivative (*R*)-**7** was transformed at  $314 \text{ pmol min}^{-1} \text{mg}^{-1}$ . Hence, the introduction of the methyl group into (*R*)-**6** yielding (*R*)-**7** corresponded to a  $\sim 5$ -fold enhanced glucuronidation rate, whereas for the respective (*S*)-enantiomers the conjugation rate was only doubled (Table 2). The increase in the ER induced by the methylation of (*R*)-**6** and (*S*)-**6** yielding (*R*)-**7** and (*S*)-**7**, respectively, was equal to the ratio of the resulting changes in glucuronidation rates, in this example 5 divided by 2. In general, shifts to higher stereoselectivities were observed when the introduction or the exchange of functional groups induced only a small increase (high decrease) in the glucuronidation rate for (*S*)-enantiomers ( $v_{\text{S}}$ ) accompanied by a higher increase (smaller decrease) in the conjugation rate for the respective (*R*)-enantiomers ( $v_{\text{R}}$ ). Therefore, structure–activity relationships (SARs) with respect to the diastereoselectivity of the GlcA-transfer reaction were derived by relating

**Table 2.** Velocities and Eudismic Ratios for the Enantiomerically Pure Alcohols

compd	UGT2B7			UGT2B17		
	$v_R^a$ pmol min <sup>-1</sup> mg <sup>-1</sup>	$v_S^b$ pmol min <sup>-1</sup> mg <sup>-1</sup>	ER <sup>c</sup>	$v_R^a$ pmol min <sup>-1</sup> mg <sup>-1</sup>	$v_S^b$ pmol min <sup>-1</sup> mg <sup>-1</sup>	ER <sup>c</sup>
1	29.5	3.56	8.29	56.8	1.30	43.7
2	139	9.60	14.5	83.6	1.40	59.7
3	64.5	1.11	58.1	54.1	1.20	45.1
4	269	32.1	8.38	92.2	5.28	17.5
5	253	38.5	6.57	460	1.80	256
6	28.4	4.45	6.38	60.8	1.21	50.2
7	114	2.93	38.9	314	2.40	131
8	5.71	2.10	2.72	12.5	1.10	11.4
9	29.1	5.03	5.79	28.4	1.99	14.3
10	41.2	6.01	6.86	219	2.01	109
11	30.5	27.8	1.10	18.8	1.34	14.0
12	23.0	3.05	7.54	54.3	3.90	13.9
13	17.8	3.90	4.56	10.6	1.29	8.22
14	ND <sup>d</sup>	ND <sup>d</sup>	<i>d</i>	ND <sup>d</sup>	ND <sup>d</sup>	<i>d</i>

<sup>a</sup> Glucuronidation rate for the (*R*)-enantiomer. SD, CI<sub>95%</sub>, and *R*<sup>2</sup> are included in the Supporting Information. <sup>b</sup> Glucuronidation rate for the (*S*)-enantiomer. SD, CI<sub>95%</sub>, and *R*<sup>2</sup> are included in the Supporting Information. <sup>c</sup> The eudismic ratio (ER) was calculated by dividing  $v_R$  by  $v_S$ . <sup>d</sup> The [<sup>14</sup>C]glucuronide was not detected (ND) and, therefore, the respective ER was not calculated.

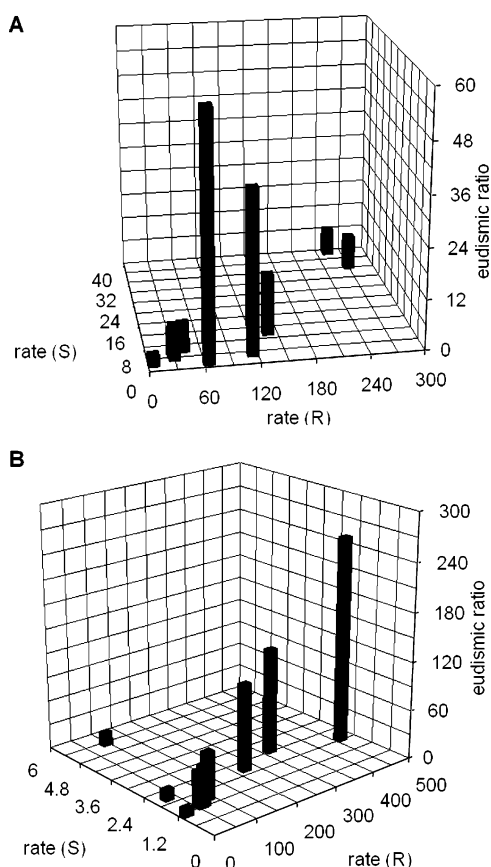


**Figure 3.** Correlation between the ER,  $v_R$ , and  $v_S$  for the alcohols 1–10: (A) UGT2B7; (B) UGT2B17. For UGT2B17 it was observed that the stereoselectivity increased with increasing  $v_R$  values accompanied by minor changes, or even no variations, in the respective  $v_S$  values (B). In the case of UGT2B7, however, the highest ERs were obtained for compounds displaying moderate  $v_R$  values and small  $v_S$  values (A).

the changes in glucuronidation rates for a pair of structurally related (*R*)- and (*S*)-enantiomers to changes in their substitution pattern. The three-dimensional plot in Figure 3 relates the measured velocities,  $v_R$  and  $v_S$ , to the respective ERs. For UGT2B17, a clear trend was observed, insofar as the increase in the ER was caused by a sharp increase in  $v_R$  accompanied by an approximately constant  $v_S$  (Figure 3). Therefore, in the case of UGT2B17, the highest ERs were associated with the

highest  $v_R$  values. For UGT2B7, however, the increase in stereoselectivity resulted either from the decrease in  $v_R$  accompanied by a higher decrease in  $v_S$  or from an increase in  $v_R$  with an approximately constant  $v_S$ . Therefore, the highest ERs were associated with compounds displaying low  $v_S$  and moderate  $v_R$  values (Figure 3).

The SARs for the UGT2B17-catalyzed glucuronidation were derived by relating the substitution pattern of the bicyclic alcohols 1–10 to their stereoselectivities and conjugation rates, on the basis of the principles outlined in detail above (Figure 3). The methylated alcohols 5, 7, and 10 displayed the highest ERs, ranging from 109 to 256 (Table 2). The common characteristic of these alcohols was the methyl group attached to carbon atom 7 in the case of compound 5 and to carbon atom 6 in the case of the indanol derivative 5 and chromanol derivative 7 (Figure 4). The methyl group in this particular position of the bicyclic scaffold played an important role in shifting the stereoselectivities to higher levels. This finding was derived by comparing the ERs of the methylated compounds 5, 7, and 10 to those of their unsubstituted derivatives, namely, alcohols 1, 6, and 8. The latter displayed significantly lower ERs of 43.7, 50.2, and 11.4, respectively (Table 2). Furthermore, the methyl group was superior in shifting the stereoselectivity toward higher levels compared to a methoxy group attached to the same carbon atom, because the ER of alcohol 3 was significantly smaller (45.1) compared to that of the methylated compounds 5, 7, and 10. However, the shift of the methoxy group from carbon atom 7 (compound 3) to position 5 (compound 2) had only a minor effect on both ER and  $v_R$ . The exchange of the methyl group from carbon atom 5 (compound 9) to position 7 (alcohol 10) induced a 7.6-fold increase in the respective ERs. Furthermore, the shift from the indanol derivatives 8–10 to the respective tetralol or 4-chromanol derivatives accomplished by the introduction of one additional methylene group or oxygen atom into the indanol scaffold increased the stereoselectivity of the UGT2B17-catalyzed GlcA-transfer reaction (Figure 4). The change of the tetralol scaffold to the heterocyclic 4-chromanol had only a minute effect on the stereoselectivity (compounds 1 and 6). In contrast, the attachment of the nitro group into the bicyclic system had a significant effect on the  $v_R/v_S$  ratio. In this respect, compound 4 was the only observed “outlier” within this series of bicyclic compounds because its  $v_S$  value was 3.8-fold higher than that of compound 2, and both were glucuronidated at comparable  $v_R$  (Table 2 and Figure 4). This might indicate that the nitro group exerted a significant disturbance



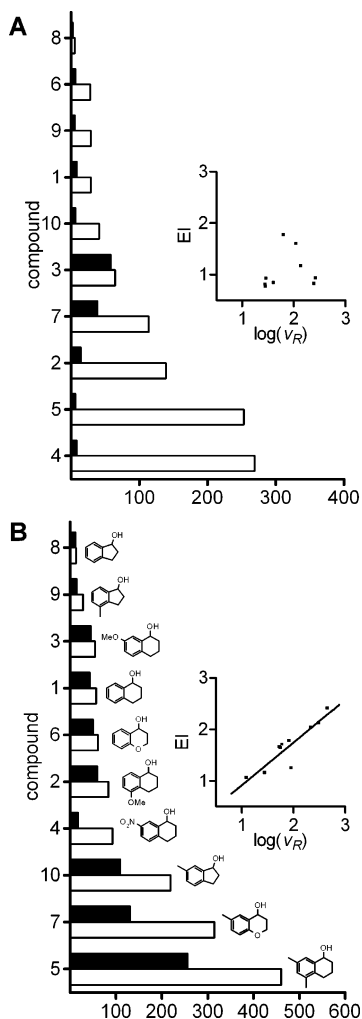


**Figure 4.** The glucuronidation rates (white bars) for the bicyclic (*R*)-enantiomers and the ERs (black bars) for the enantiomeric pairs **1–10** as determined for UGT2B7 (A) and UGT2B17 (B). The compounds were sorted by increasing velocity. In panel B, the ER increased with increasing  $v_R$ . Therefore, the (*R*)-enantiomers bearing the methyl group in *m*-position to the benzylic hydroxy function, namely (*R*)-**5**, (*R*)-**7**, and (*R*)-**10**, displayed the highest velocities and simultaneously the highest stereoselectivities. The inset shows that the EI increased with increasing  $\log(v_R)$  consistent with Pfeiffer's rule. The curve in the inset was fitted by linear regression ( $R^2 = 0.82$ ). The EAQ was  $0.83 \pm 0.14$ , indicating a strong participation of the element of chirality. Compound **4** displayed a significant deviation from the regression curve as discussed in the text. In panel A, in the case of UGT2B7, there was no clear trend for the relationship of the glucuronidation velocity and the stereoselectivity. The nitro compound **4** was the best substrate in this series accompanied by a low ER. The highest stereoselectivities were associated with compounds **3** and **7**, which were glucuronidated at moderate rates. The inset of panel A shows no correlation between the EI and  $\log(v_R)$  (violation of Pfeiffer's rule). This indicated no participation of the element of chirality in the GlcA-transfer reaction catalyzed by UGT2B7.

to the system, possibly because this residue is bulkier and possesses a higher electron density in comparison to the methyl and methoxy groups. This finding might indicate a different orientation of compound **4** within the active site of the enzyme rendering also the (*S*)-enantiomer a better substrate for UGT2B17 leading to its higher  $v_S$  value and, hence, inducing a lower level of chiral distinction during the glucuronidation reaction (Figure 4). In conclusion, even the flexible, aliphatic alcohols **11–13** were glucuronidated by UGT2B17 at pronounced diastereoselectivities, favoring the conjugation of the (*R*)-enantiomers over

their respective (*S*)-enantiomers (Table 2 and Figure 2). Therefore, the high rotational “freedom” of the hydroxy group had no significant effect on the substrate–product stereoselectivity of the GlcA-transfer step. We therefore concluded that UGT2B17 displayed high levels of chiral distinction during the glucuronidation reaction, independently of the flexibility of the chiral substrate.

In the case of UGT2B17, clear trends were observed that led to the derivation of SARs with respect to higher levels of chiral distinction. For UGT2B7, however, no comparable pattern was found (Figure 4), but some valid conclusions could nevertheless be made. In contrast to UGT2B17, the compounds **2**, **4**, and **5**, displaying the highest  $v_R$  values, did not exhibit the highest stereoselectivities during the UGT2B7-catalyzed conjugation reaction (Table 2, Figures 3 and 4). Instead, the highest ERs were associated with compounds **3** and **7**, displaying moderate  $v_R$  and small  $v_S$  values (Table 2 and Figure 3). In this respect, within the set of the tetralol derivatives **1–5**, the introduction of the methoxy group in position 7 (compound **3**) caused a clear shift to higher ERs, primarily induced by the decrease in  $v_S$  (Table 2 and Figure 3). However, the increase in  $v_R$  was accompanied by an analogous change to higher  $v_S$  values, as indicated by similar ERs for 6 out of 8 bicyclic alcohols, ranging from 5.79 to 14.5, corresponding to an increase in the stereoselectivity of at most 2.5-fold (Table 2, Figures 3 and 4).

The relationship between  $v_R$  and ER is presented in Figure 4. It can be seen from the inset that in the case of UGT2B17 the data obeyed Pfeiffer's rule, stating that the higher the activity is of the eutomer the higher the separation is in activities between eutomer and distomer.<sup>38</sup> Correlation analysis afforded a clear relationship between these two parameters (Pearson  $r = 0.904$ , two-tailed  $P = 3.0 \times 10^{-4}$ ,  $\alpha = 0.05$ ), showing that the eudismic index (EI), defined as  $\log(v_R/v_S)$ , increased linearly toward higher velocities for the eutomer,  $\log(v_R)$  (Figure 4). The determination of the slope of this straight line by linear regression yielded the eudismic activity quotient (EAQ) of  $0.83 \pm 0.14$  (Figure 4). This value quantifies the rate of change in the EI with velocity. This high EAQ strongly indicated a significant participation of the element of chirality during the glucuronidation reaction catalyzed by UGT2B17. We therefore concluded that the two enantiomers of each compound displayed high similarities in their orientation within the active site of UGT2B17. With both enantiomers taking the same arrangement, the hydroxy group of the (*S*)-enantiomer was unfavorably placed (“out of reach”) for efficient GlcA-transfer, resulting in constantly low  $v_S$  values. On the other hand, the (*R*)-enantiomers were conjugated rapidly; hence, the respective hydroxy group was favorably placed within the catalytic site, resulting in a fast GlcA-transfer ( $v_R \gg v_S$ ). In the case of UGT2B7, however, the obtained data violated Pfeiffer's rule, insofar as there was no correlation between the EI and  $\log(v_R)$ . Instead, the data points seemed to be randomly scattered within the limits of the two parameters (Figure 4). This lack of correlation showed that factors other than the spatial arrangement of the hydroxy group became dominant, suggesting that the element of chirality did not significantly participate in the GlcA-transfer reaction catalyzed by UGT2B7. The two enantiomers of each compound seemed, therefore, to display distinct orientations within the active site, meaning that the catalytic site of UGT2B7 allowed for the different arrangement of the (*R*)- and its respective (*S*)-enantiomer during the actual transfer reaction. This conclusion was supported by the result that the two enantiomers of the flexible compound **11** were glucuronidated at similar rates, and therefore, the respective ER was close to unity (Table 2 and

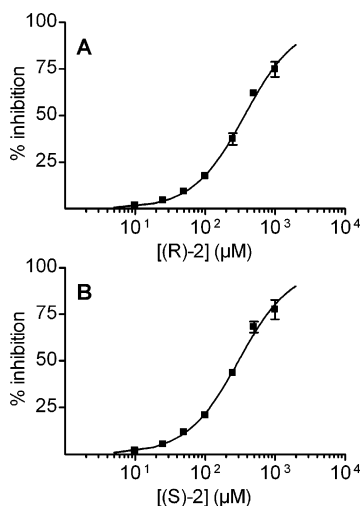


**Figure 5.** Semilogarithmic concentration–response plot for the inhibition assays using (*R*)-**2** (A) and (*S*)-**2** (B). Both were assayed with UGT2B7. Scopoletin was used as the substrate at a concentration similar to its  $K_m$  for that enzyme (500  $\mu\text{M}$ ). The reaction assay contained 5.0 mM cosubstrate (UDPGlcA), and the protein concentration was 0.10  $\mu\text{g}/\mu\text{L}$  (incubation time of 15 min). The  $\text{IC}_{50}$  for (*R*)-**2** was  $366 \pm 10 \mu\text{M}$  ( $\text{CI}_{95\%} = 345\text{--}388$ ) and  $301 \pm 10 \mu\text{M}$  for (*S*)-**2** ( $\text{CI}_{95\%} = 280\text{--}322$ ).

Figure 2). Nevertheless, the (*R*)-enantiomers were arranged more favorably during the GlcA-transfer step than their corresponding stereoisomers because they were conjugated at higher rates than their respective (*S*)-enantiomers ( $v_R \geq v_S$ ).

In the preceding sections we have discussed the influences of the element of chirality on the actual GlcA-transfer reaction, and we will now turn to its effect on the formation of the enzyme–substrate complex. It was asked whether the preferred glucuronidation of (*R*)-enantiomers over their corresponding (*S*)-enantiomers by both UGT2B7 and UGT2B17 resulted from vast differences in their affinities toward these enzymes. To answer this question, we employed the  $\text{IC}_{50}$  value as a measure for the affinity toward the enzymes. The  $\text{IC}_{50}$  is correlated to its  $K_i$  by the equations derived by Cheng and Prusoff, and it therefore relates to the dissociation (formation) of the enzyme–inhibitor complex.<sup>39</sup> This complex is called here the enzyme–substrate complex because the inhibitors, i.e., the enantiomers of compounds **1–13**, are substrates of the enzymes (the so-called “second substrates” in the inhibition assay). Scopoletin was chosen as the “first-substrate” because its glucuronide was conveniently identified by fluorescence detection and the  $K_m$  values of this substrate toward UGT2B7 and UGT2B17 (531 and 309  $\mu\text{M}$ , respectively) were optimal for the  $\text{IC}_{50}$  determination for the bicyclic enantiomeric alcohols **1–10** at a scopoletin concentration identical to its  $K_m$  (Figure 5). However, the measurement at a scopoletin concentration resembling its  $K_m$  was not possible in the case of the aliphatic alcohols **11–13** because of their low solubilities. Therefore, the scopoletin concentration was lowered to 50  $\mu\text{M}$  to obtain meaningful  $\text{IC}_{50}$  values for these lipophilic alcohols. It should be mentioned here that the  $\text{IC}_{50}$  values for the enantiomers of compounds **11–13** were not comparable to the values for compounds **1–10**, because the  $\text{IC}_{50}$  depends on the scopoletin concentration. However, the values within each set of compounds—alcohols **1–10** and **11–13**—could be compared to each other. Compound **14** was excluded from this study because it was not a substrate of both enzymes.

The results of the inhibition assays are presented in Table 3. As can be seen from the data, the  $\text{IC}_{50}$  values for the enantiomers

**Table 3.**  $\text{IC}_{50}$  Values for the Enantiomerically Pure Enantiomers

compd	UGT2B7 <sup>a</sup>		UGT2B17 <sup>b</sup>	
	$\text{IC}_{50}$ ( <i>R</i> ) ( $\mu\text{M}$ ) <sup>c</sup>	$\text{IC}_{50}$ ( <i>S</i> ) ( $\mu\text{M}$ ) <sup>c</sup>	$\text{IC}_{50}$ ( <i>R</i> ) ( $\mu\text{M}$ ) <sup>c</sup>	$\text{IC}_{50}$ ( <i>S</i> ) ( $\mu\text{M}$ ) <sup>c</sup>
<b>1</b>	337 ± 8	489 ± 14	242 ± 7	374 ± 10
<b>2</b>	366 ± 10	301 ± 10	112 ± 3	132 ± 3
<b>3</b>	284 ± 9	351 ± 5	162 ± 5	216 ± 13
<b>4</b>	599 ± 26	651 ± 10	217 ± 4	305 ± 14
<b>5</b>	158 ± 4	166 ± 8	144 ± 6	98 ± 4
<b>6</b>	507 ± 23	518 ± 7	448 ± 10	319 ± 8
<b>7</b>	225 ± 10	182 ± 6	365 ± 8	325 ± 11
<b>8</b>	275 ± 8	513 ± 14	517 ± 10	545 ± 21
<b>9</b>	317 ± 8	179 ± 7	682 ± 15	608 ± 20
<b>10</b>	394 ± 11	540 ± 13	489 ± 5	728 ± 15
<b>11<sup>d</sup></b>	130 ± 7	214 ± 15	389 ± 14	537 ± 40
<b>12<sup>d</sup></b>	79 ± 3	105 ± 4	578 ± 23	657 ± 27
<b>13<sup>d</sup></b>	344 ± 10	532 ± 27	703 ± 46	606 ± 21

<sup>a</sup> Assayed with 500  $\mu\text{M}$  scopoletin ( $K_m = 531 \mu\text{M}$ ). <sup>b</sup> Assayed with 300  $\mu\text{M}$  scopoletin ( $K_m = 309 \mu\text{M}$ ). <sup>c</sup> The mean value ± standard deviation is displayed. The  $\text{CI}_{95\%}$ ,  $R^2$ , and the Hill coefficient are included in Supporting Information. <sup>d</sup> The enantiomers were only employed at concentrations ranging from 5 to 100  $\mu\text{M}$ , because of their low solubilities. The concentration of the substrate scopoletin was lowered to 50  $\mu\text{M}$ , because of the high  $\text{IC}_{50}$  values and the low maximum concentrations of these compounds. This renders the  $\text{IC}_{50}$  value incomparable to the values obtained for the bicyclic enantiomers **1–10**.

of each compound toward the UGTs 2B7 and 2B17 were of the same order of magnitude and even nearly identical.<sup>40</sup> Plots of the  $\text{IC}_{50}$  values of the (*S*)-enantiomers versus the  $\text{IC}_{50}$  values of the (*R*)-enantiomers are presented in Figure 6. The affinities of a pair of enantiomers toward both enzymes were rather similar because the data points were distributed near to the bisecting line (Figure 6). The ERs of the  $\text{IC}_{50}$  values for UGT2B7 ranged between 1.1 and 1.9, and those for UGT2B17 were between 1.0 and 1.6 (Figure 6). Furthermore, we observed no general bias toward (*R*)- or (*S*)-enantiomers because the data points were scattered randomly below and above the bisecting line. These results were confirmed by measuring the  $\text{IC}_{50}$  values of each racemic mixture of the compounds **5**, **7**, and **10**, and the results showed that the potency of each racemate was intermediary between the two respective enantiomers (results not shown). The inset in Figure 6 revealed the lack of correlation between the EI and the affinity of the eutomer toward both UGT2B7 and UGT2B17, a violation of Pfeiffer’s rule. These findings indicated that the element of chirality did not significantly participate during the formation of the enzyme–substrate complex. However, these findings could also have been a result of unspecific, noncompetitive, and uncompetitive binding to the enzymes, blurring the stereoselectivities of the active-site directed, competitive interaction. Therefore, we determined the mechanism of inhibition for the racemates of compounds **5**, **7**, and **10** by the direct plot method and simultaneous nonlinear regression analysis (velocity versus scopoletin concentration). The data were fitted to the competitive, noncompetitive, mixed-type, and uncompetitive inhibition models. The different models were ranked according to the corrected Akaike’s information criterion ( $\text{AIC}_c$ ). On the basis of these results, the active-site directed, competitive inhibition model was chosen and the resulting  $K_{ic}$  values were in good agreement with those calculated from the respective  $\text{IC}_{50}$  values by the Cheng–Prusoff equation (Figure 7 and Supporting Information). Therefore, we assumed that the spatial arrangement of the hydroxy group had indeed no effect on the affinity toward the enzymes. This might indicate that the nucleophilic hydroxy group was negligible during the formation of the enzyme–substrate complex, meaning that the enzyme merely recognized the lipophilic core of the structure. The (*R*)- and its respective (*S*)-enantiomer displayed very similar affinities toward both UGTs 2B7 and

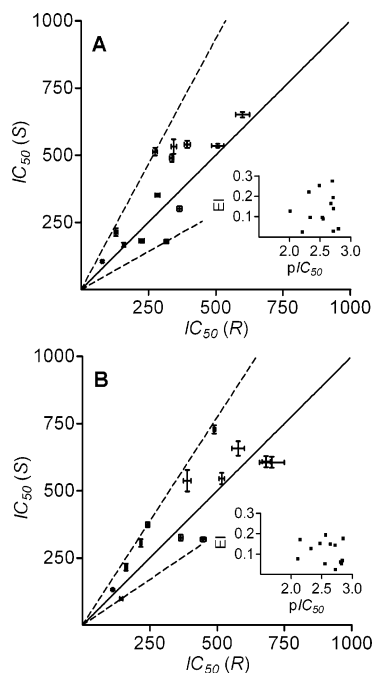


**Figure 6.**  $IC_{50}$  values of the (S)-enantiomers versus the  $IC_{50}$  values of the respective (R)-enantiomers of compounds 1–13. Panel A displays the data for UGT2B7, and panel B shows the results for UGT2B17. The bisecting solid line corresponds to a  $IC_{50}$  ratio of unity. Data points on this line represent identical  $IC_{50}$  values for the (R)- and (S)-enantiomer. Points above the bisecting line indicate a higher affinity for the (S)-enantiomer toward the enzyme, and points below the bisecting line indicate bias toward (R)-enantiomers. The slopes of the dashed lines represent the maximal and minimal  $IC_{50}$  ratios corresponding to the maximal bias toward the (S)-enantiomer and the maximal bias toward the (R)-enantiomer, respectively. The error bars represent the standard deviations as presented in Table 3. The insets of panels A and B display the lack of correlation between the EI and the  $pIC_{50}$  for both enzymes (violation of Pfeiffer's rule) indicating no significant participation of the element of chirality during the formation of the enzyme–enantiomer complex.

2B17, and therefore, the enzymes displayed no significant chiral distinction during the formation of the enzyme–substrate complex. Hence, the binding site of UGT2B7 and UGT2B17 seemed to be quite “flexible” in accepting the enantiomers of each compound at similar affinities, and it may be concluded that the preferential glucuronidation of the (R)-enantiomers by the UGTs 2B7 and 2B17 did not result from differences in the affinities toward the enzymes.

Interestingly, the results of the affinity assays were in sharp contrast to the findings of the glucuronidation assays. Both enzymes displayed diastereoselective conjugation favoring the (R)- over its respective (S)-enantiomer at eudismic ratios up to 256. In contrast, the formation of the enzyme–substrate complex was not influenced by the spatial arrangement of the hydroxy group, because the enzymes accepted the stereoisomers at very similar affinities. This study showed that the observed stereoselectivities resulted from the preferential conjugation of the (R)- over its (S)-enantiomer during the catalytic transfer reaction per se and not from distinct affinities between the stereoisomers to the enzymes.

## Conclusion

To date, studies on metabolic enzymes such as UGTs, sulfotransferases, and acyltransferases employing whole sets of chiral compounds have not been conducted.<sup>2</sup> This lack of eudismic data is probably due to the general conception that these enzymes are quite “flexible” in nature and, therefore, do

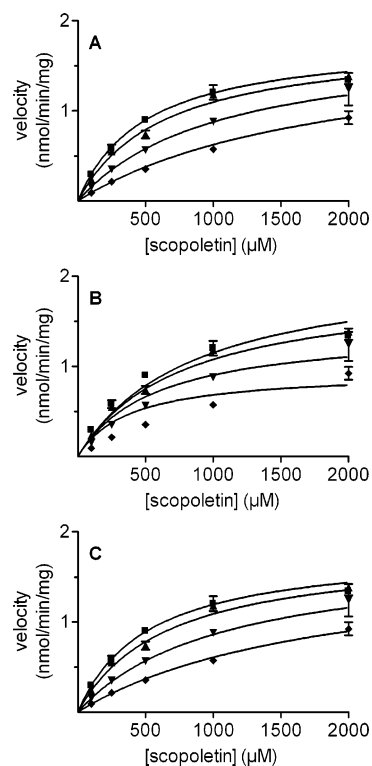


**Figure 7.** Inhibition of the UGT2B7-catalyzed scopoletin glucuronidation by *rac*-5. The data were fitted by simultaneous nonlinear regression (global fitting) to the competitive (A), uncompetitive (B), mixed-type (C), and noncompetitive inhibition models. The noncompetitive model did not converge. Model comparison was carried out by employing the corrected Akaike's information criterion ( $AIC_C$ ). The  $AIC_C$  values were  $-313$ ,  $-262$ , and  $-311$  for the competitive, uncompetitive, and mixed-type model, respectively. The evidence ratios showed that the competitive inhibition model was  $\sim 12 \times 10^{10}$  times more likely than uncompetitive inhibition and  $\sim 2.7$  times more likely than mixed-type inhibition. In addition, the mixed-type inhibition model yielded a very high and therefore negligible uncompetitive inhibition constant ( $K_{iu}$ ) of  $\sim 2.1 \times 10^3 \mu$ M, whereas its competitive inhibition constant ( $K_{ic}$ ) was similar to that obtained for competitive inhibition ( $\sim 100 \mu$ M). On the basis of these results, competitive inhibition was chosen to be most likely to explain the data correctly (cf. Supporting Information).

not display high levels of chiral distinction. In this study, however, we showed that in particular UGT2B17 was highly stereoselective in its glucuronidation reaction and the “flexibility” was merely limited to the formation of the enzyme–substrate complex. Therefore, also enzymes of the human metabolic system are capable of displaying high levels of substrate–product stereoselectivity. In addition, the findings of this study suggest that eudismic analysis may be used to edge closer to understanding the mechanism of the UGT-catalyzed glucuronidation reaction at the molecular level.

## Experimental Section

**Materials.** UDPGlcA (trisodium salt, CAS 63700-19-6), scopoletin (CAS 92-61-5), and saccharic acid-1,4-lactone (CAS 61278-30-6) were obtained from Sigma (St. Louis, MO). [ $^{14}$ C]UDPGlcA was acquired from PerkinElmer Life and Analytical Sciences (Boston, MA). HPLC grade solvents were used throughout the study. The recombinant human UGT2B7 was expressed in baculovirus-infected insect cells as previously described.<sup>41</sup> The cDNA for the human UGT2B17 was a generous gift from Prof. Peter Mackenzie (Flinders University, Flinders Medical Centre, Bedford Park, South Australia, Australia), and it was also expressed as a His-tagged protein in insect cells. 5-Methoxy-1-tetralone (CAS 33892-75-0), 7-methoxy-1-tetralone (CAS 6836-19-7), 5,7-dimethyl-1-tetralone (CAS 13621-25-5), 4-chromanone (CAS 491-37-2),



6-methyl-4-chromanone (CAS 39513-75-2), 4-methyl-1-indanone (CAS 24644-78-8), 6-methyl-1-indanone (CAS 24623-20-9), 1'-acetonaphthone (CAS 941-98-0), 2'-acetonaphthone (CAS 93-08-3), 9-acetylanthracene (CAS 784-04-3), 9-acetylphenanthrene (CAS 2039-77-2), borane *N,N*-diethylaniline complex (CAS 13289-97-9), and anhydrous toluene were acquired from Aldrich (Schnellendorf, Germany). 7-Nitro-1-tetralone (CAS 40353-34-2) was purchased from Alfa Aesar/Lancaster (Lancashire, U.K.).

**Analytcs.** The progress of chemical reactions was monitored by thin-layer chromatography on silica gel 60-F<sub>254</sub> plates acquired from Merck (Darmstadt, Germany). Optical purities were determined applying HPLC by use of a chiral (*R,R*)-ULMO column (25 cm × 4.6 mm; Regis Technologies, Morton Grove, IL). The eluent consisted of 2-propanol in *n*-hexane, and signal detection was conducted at 254 nm. Melting points were measured using an IA9100 digital melting point apparatus (Electrothermal Engineering, Essex, U.K.). The synthesized compounds were analyzed by NMR on a Varian Mercury 300 MHz spectrometer (Varian, Palo Alto, CA) and by GC-MS. The GC-MS system consisted of a 5890A gas chromatograph and a 5970 mass selective detector (Hewlett-Packard, Palo Alto, CA). NMR spectra were processed using the Varian VNMR software (Varian, Palo Alto, CA) on a UNIX Solaris workstation. GC-MS spectra were analyzed with the HP ChemStation program on a Windows 3.1 workstation. Optical rotatory powers were determined with a Polartronic E polarimeter by use of a microtube for small sample volumes (100 mL, 1.10 mL; Schmidt + Haensch, Berlin, Germany). The elemental analyses were conducted by Robertson-Microlit Laboratories (Madison, NJ).

The HPLC system consisted of the Agilent 1100 series degasser, binary pump, autosampler, thermostated column compartment (sustained at 40 °C), multiple wavelength detector, fluorescence detector, and fraction collector (Agilent Technologies, Palo Alto, CA). Radiolabeled [<sup>14</sup>C]glucuronides were detected by use of a 9701 HPLC radioactivity monitor (Reeve Analytical, Glasgow, Scotland) at 16 kcounts/s after separation on a Hypersil BDS-C18 column (4.6 mm × 150 mm; Agilent Technologies, Palo Alto, CA) with the use of a mixture of methanol and phosphate buffer (50 mM, pH 3) as an eluent. Signal separation for the scopoletin assays was carried out using a reversed-phase C18 column (Chromolith SpeedROD RP18e 50 mm × 4.6 mm; Merck, Darmstadt, Germany). The resulting spectra were analyzed with Agilent ChemStation software (revision B.01.01) on a Windows 2000 workstation. Regression and correlation analyses were conducted using Prism4 software (version 4.02; GraphPad Software, San Diego, CA).

**General Procedure for the CBS Reduction.** All reactions were performed in oven-dried glassware under an atmosphere of dry argon. (*R*)- and (*S*)-2-(diphenylhydroxymethyl)pyrrolidine were synthesized as previously described.<sup>24</sup>

To a solution of (*R*)- or (*S*)-2-(diphenylhydroxymethyl)pyrrolidine (253 mg, 1.00 mmol) in dry toluene (10.0 mL) was added trimethyl borate (125 mg, 1.20 mmol), and the mixture was stirred under argon atmosphere at room temperature for 2 h (23 °C). Borane *N,N*-diethylaniline complex (1.78 mL, 10.0 mmol) was added via cannula, followed by dropwise addition of a solution of ketone (10.0 mmol) in dry toluene (10.0 mL) over 2.5 h with a syringe pump. The mixture was stirred overnight at room temperature. The resulting solution was quenched with methanol (5.0 mL) at 0 °C and concentrated under reduced pressure. The residue was purified by flash chromatography on a silica gel Flash 25+M cartridge (25 × 150 mm) with a SP4 purification system (Biotage AB, Uppsala, Sweden; 50 mL/min flow rate, detection at 254 nm). The eluent consisted of a mixture of ethyl acetate and *n*-hexane (cf. Supporting Information). Subsequently, the eluent was evaporated in vacuo and the resulting solid was recrystallized several times to increase the enantiomeric excess. The obtained crystals were filtered, washed with *n*-hexane, and dried in vacuo. In the case of liquid compounds, the enantiomers were resolved by HPLC purification on an (*R,R*)-ULMO column. The enantiomers of compounds **1** and **8** were prepared according to the procedure as previously described.<sup>24</sup>

**(R)-2: (-)-(R)-5-Methoxy-1-tetralol.**  $R_f = 0.28$  (15% EtOAc in *n*-hexane); mp 97.5–97.9 °C (toluene/*n*-hexane);  $[\alpha]_D^{23} -17.3$  deg·mL·dm<sup>-1</sup>·g<sup>-1</sup> (*c* 1.5, CHCl<sub>3</sub>). Anal. (C<sub>11</sub>H<sub>14</sub>O<sub>2</sub>) C, H.

**(S)-2: (+)-(S)-5-Methoxy-1-tetralol.**  $R_f = 0.28$  (15% EtOAc in *n*-hexane); mp 97.8–98.2 °C (toluene/*n*-hexane);  $[\alpha]_D^{23} +16.9$  deg·mL·dm<sup>-1</sup>·g<sup>-1</sup> (*c* 1.5, CHCl<sub>3</sub>). Anal. (C<sub>11</sub>H<sub>14</sub>O<sub>2</sub>) C, H.

**(R)-3: (-)-(R)-7-Methoxy-1-tetralol.**  $R_f = 0.24$  (20% EtOAc in *n*-hexane); mp 45.7–46.4 °C (toluene/*n*-hexane);  $[\alpha]_D^{23} -45.4$  deg·mL·dm<sup>-1</sup>·g<sup>-1</sup> (*c* 1.5, CHCl<sub>3</sub>). Anal. (C<sub>11</sub>H<sub>14</sub>O<sub>2</sub>) C, H.

**(S)-3: (+)-(S)-7-Methoxy-1-tetralol.**  $R_f = 0.24$  (20% EtOAc in *n*-hexane); mp 46.0–46.5 °C (toluene/*n*-hexane);  $[\alpha]_D^{23} +47.3$  deg·mL·dm<sup>-1</sup>·g<sup>-1</sup> (*c* 1.5, CHCl<sub>3</sub>). Anal. (C<sub>11</sub>H<sub>14</sub>O<sub>2</sub>) C, H.

**(R)-4: (-)-(R)-7-Nitro-1-tetralol.**  $R_f = 0.31$  (25% EtOAc in *n*-hexane); mp 79.9–80.6 °C (CH<sub>2</sub>Cl<sub>2</sub>/*n*-hexane);  $[\alpha]_D^{23} -63.7$  deg·mL·dm<sup>-1</sup>·g<sup>-1</sup> (*c* 1.5, CHCl<sub>3</sub>). Anal. (C<sub>10</sub>H<sub>11</sub>NO<sub>3</sub>) C, H, N.

**(S)-4: (+)-(S)-7-Nitro-1-tetralol.**  $R_f = 0.31$  (25% EtOAc in *n*-hexane); mp 80.2–80.8 °C (CH<sub>2</sub>Cl<sub>2</sub>/*n*-hexane);  $[\alpha]_D^{23} +62.3$  deg·mL·dm<sup>-1</sup>·g<sup>-1</sup> (*c* 1.5, CHCl<sub>3</sub>). Anal. (C<sub>10</sub>H<sub>11</sub>NO<sub>3</sub>) C, H, N.

**(R)-5: (-)-(R)-5,7-Dimethyl-1-tetralol.**  $R_f = 0.26$  (10% EtOAc in *n*-hexane); mp 87.5–88.0 °C (10% EtOAc in *n*-hexane);  $[\alpha]_D^{23} -48.5$  deg·mL·dm<sup>-1</sup>·g<sup>-1</sup> (*c* 1.5, CHCl<sub>3</sub>). Anal. (C<sub>12</sub>H<sub>16</sub>O) C, H.

**(S)-5: (+)-(S)-5,7-Dimethyl-1-tetralol.**  $R_f = 0.28$  (10% EtOAc in *n*-hexane); mp 87.4–88.0 °C (CH<sub>2</sub>Cl<sub>2</sub>/*n*-hexane);  $[\alpha]_D^{23} +49.4$  deg·mL·dm<sup>-1</sup>·g<sup>-1</sup> (*c* 1.5, CHCl<sub>3</sub>). Anal. (C<sub>12</sub>H<sub>16</sub>O) C, H.

**(R)-6: (+)-(R)-4-Chromanol.**  $R_f = 0.26$  (15% EtOAc in *n*-hexane); mp 76.2–76.7 °C (toluene/*n*-hexane);  $[\alpha]_D^{23} +46.0$  deg·mL·dm<sup>-1</sup>·g<sup>-1</sup> (*c* 1.5, CHCl<sub>3</sub>). Anal. (C<sub>9</sub>H<sub>10</sub>O<sub>2</sub>) C, H.

**(S)-6: (-)-(S)-4-Chromanol.**  $R_f = 0.25$  (15% EtOAc in *n*-hexane); mp 76.2–76.6 °C (toluene/*n*-hexane);  $[\alpha]_D^{23} -43.9$  deg·mL·dm<sup>-1</sup>·g<sup>-1</sup> (*c* 1.5, CHCl<sub>3</sub>). Anal. (C<sub>9</sub>H<sub>10</sub>O<sub>2</sub>) H, C: calcd, 71.98; found, 71.22.

**(R)-7: (+)-(R)-6-Methyl-4-chromanol.**  $R_f = 0.27$  (20% EtOAc in *n*-hexane); mp 84.3–84.9 °C (CH<sub>2</sub>Cl<sub>2</sub>/*n*-hexane);  $[\alpha]_D^{23} +37.5$  deg·mL·dm<sup>-1</sup>·g<sup>-1</sup> (*c* 1.5, CHCl<sub>3</sub>). Anal. (C<sub>10</sub>H<sub>12</sub>O<sub>2</sub>) C, H.

**(S)-7: (-)-(S)-6-Methyl-4-chromanol.**  $R_f = 0.27$  (20% EtOAc in *n*-hexane); mp 83.9–84.4 °C (CH<sub>2</sub>Cl<sub>2</sub>/*n*-hexane);  $[\alpha]_D^{23} -38.6$  deg·mL·dm<sup>-1</sup>·g<sup>-1</sup> (*c* 1.5, CHCl<sub>3</sub>). Anal. (C<sub>10</sub>H<sub>12</sub>O<sub>2</sub>) C, H.

**(R)-9: (-)-(R)-4-Methyl-1-indalol.**  $R_f = 0.29$  (20% EtOAc in *n*-hexane); mp 69.3–69.8 °C (20% EtOAc in *n*-hexane);  $[\alpha]_D^{23} -36.3$  deg·mL·dm<sup>-1</sup>·g<sup>-1</sup> (*c* 1.5, CHCl<sub>3</sub>). Anal. (C<sub>10</sub>H<sub>12</sub>O) C, H.

**(S)-9: (+)-(S)-4-Methyl-1-indalol.**  $R_f = 0.31$  (20% EtOAc in *n*-hexane); mp 69.0–69.6 °C (CH<sub>2</sub>Cl<sub>2</sub>/*n*-hexane);  $[\alpha]_D^{23} +36.6$  deg·mL·dm<sup>-1</sup>·g<sup>-1</sup> (*c* 1.5, CHCl<sub>3</sub>). Anal. (C<sub>10</sub>H<sub>12</sub>O) C, H.

**(R)-10: (-)-(R)-6-Methyl-1-indalol.**  $R_f = 0.23$  (15% EtOAc in *n*-hexane); mp 94.6–95.7 °C (CH<sub>2</sub>Cl<sub>2</sub>/*n*-hexane);  $[\alpha]_D^{23} -32.3$  deg·mL·dm<sup>-1</sup>·g<sup>-1</sup> (*c* 1.5, CHCl<sub>3</sub>). Anal. (C<sub>10</sub>H<sub>12</sub>O) C, H.

**(S)-10: (+)-(S)-6-Methyl-1-indalol.**  $R_f = 0.25$  (15% EtOAc in *n*-hexane); mp 94.0–95.0 °C (CH<sub>2</sub>Cl<sub>2</sub>/*n*-hexane);  $[\alpha]_D^{23} +31.3$  deg·mL·dm<sup>-1</sup>·g<sup>-1</sup> (*c* 1.5, CHCl<sub>3</sub>). Anal. (C<sub>10</sub>H<sub>12</sub>O) C, H.

**(R)-11: (+)-(R)-1-Naphthalen-1-ylethanol.**  $R_f = 0.21$  (10% EtOAc in *n*-hexane);  $[\alpha]_D^{23} +62.7$  deg·mL·dm<sup>-1</sup>·g<sup>-1</sup> (*c* 1.5, CHCl<sub>3</sub>). Anal. (C<sub>12</sub>H<sub>12</sub>O) C, H.

**(S)-11: (-)-(S)-1-Naphthalen-1-ylethanol.**  $R_f = 0.21$  (10% EtOAc in *n*-hexane);  $[\alpha]_D^{23} -61.2$  deg·mL·dm<sup>-1</sup>·g<sup>-1</sup> (*c* 1.5, CHCl<sub>3</sub>). Anal. (C<sub>12</sub>H<sub>12</sub>O) C, H.

**(R)-12: (+)-(R)-1-Naphthalen-2-ylethanol.**  $R_f = 0.23$  (15% EtOAc in *n*-hexane); mp 69.7–70.4 °C (CH<sub>2</sub>Cl<sub>2</sub>/*n*-hexane);  $[\alpha]_D^{23} +51.1$  deg·mL·dm<sup>-1</sup>·g<sup>-1</sup> (*c* 1.5, CHCl<sub>3</sub>). Anal. (C<sub>12</sub>H<sub>12</sub>O) C, H.

**(S)-12: (-)-(S)-1-Naphthalen-2-ylethanol.**  $R_f = 0.22$  (15% EtOAc in *n*-hexane); mp 70.1–70.7 °C (CH<sub>2</sub>Cl<sub>2</sub>/*n*-hexane);  $[\alpha]_D^{23} -49.9$  deg·mL·dm<sup>-1</sup>·g<sup>-1</sup> (*c* 1.5, CHCl<sub>3</sub>). Anal. (C<sub>12</sub>H<sub>12</sub>O) C, H.

**(R)-13: (+)-(R)-1-Anthracen-9-ylethanol.**  $R_f = 0.29$  (20% EtOAc in *n*-hexane); mp 120.6–121.5 °C (10% EtOAc in *n*-hexane);  $[\alpha]_D^{23} +13.0$  deg·mL·dm<sup>-1</sup>·g<sup>-1</sup> (*c* 1.5, CHCl<sub>3</sub>). Anal. (C<sub>16</sub>H<sub>14</sub>O) C, H.

**(S)-13: (-)-(S)-1-Anthracen-9-ylethanol.**  $R_f = 0.29$  (20% EtOAc in *n*-hexane); mp 120.6–121.5 °C (10% EtOAc in *n*-hexane);  $[\alpha]_D^{23} -13.7$  deg·mL·dm<sup>-1</sup>·g<sup>-1</sup> (*c* 1.5, CHCl<sub>3</sub>). Anal. (C<sub>16</sub>H<sub>14</sub>O) C, H.



**(R)-14:** (+)-**(R)-1-Phenanthren-9-ylethanol**.  $R_f = 0.32$  (30% EtOAc in *n*-hexane); mp 126.7–127.7 °C (toluene/*n*-hexane);  $[\alpha]_D^{23} +79.5$  deg·mL·dm<sup>-1</sup>·g<sup>-1</sup> (*c* 1.5, CHCl<sub>3</sub>). Anal. (C<sub>16</sub>H<sub>14</sub>O) C, H.

**(S)-14:** (–)-**(S)-1-Phenanthren-9-ylethanol**.  $R_f = 0.34$  (30% EtOAc in *n*-hexane); mp 126.4–127.2 °C (toluene/*n*-hexane);  $[\alpha]_D^{23} -76.8$  deg·mL·dm<sup>-1</sup>·g<sup>-1</sup> (*c* 1.5, CHCl<sub>3</sub>). Anal. (C<sub>16</sub>H<sub>14</sub>O) C, H.

**Racemization Study.** It was determined that the enantiomerically pure substrates did not undergo racemization under the reaction conditions of the enzyme assays. To determine the magnitude of racemization, each (*R*)-enantiomer was dissolved in methanol and diluted to a final concentration of 1 mg/mL with 50% methanol/water (v/v). To this solution, phosphate buffer (20 mM, pH 7.4) was added to a final concentration of 10% (v/v), and the mixture was sustained at 40 °C overnight. The methanol was removed under reduced pressure, and the solution was then extracted with diethyl ether. The organic phase was washed with water and brine and was evaporated in vacuo, and the residue was dissolved in a small amount of dichloromethane. The resulting solution was subjected to HPLC analysis to determine the optical purity.

**Activity Assays.** The progression curves were recorded using 20 μM radiolabeled [<sup>14</sup>C]UDPGlcA (20.0 μCi/mL, 196 mCi/mmol) in combination with 100 μM cold UDPGlcA yielding a total concentration of 120 μM of this cosubstrate.<sup>36</sup> The assay volume was 700 μL and consisted of 50 mM phosphate buffer (pH 7.4), 10 mM MgCl<sub>2</sub>, and 5.0 mM saccharic acid-1,4-lactone. The enzymes UGT2B7 and UGT2B17 were employed at 1.0 μg/μL. The enzyme reactions were initiated after 5 min of preincubation (37 °C) by the addition of a solution of the bicyclic enantiomer in 50% water/DMSO (v/v) to a final, saturating concentration of 2.0 mM. The flexible compounds **11–14** were employed at a final concentration of 0.1 mM. The DMSO concentration in the assay mixtures was 2.5% (v/v). The enzyme reactions, incubated at 37 °C, were terminated after a set amount of time by pipetting 100 μL of the reaction mixture to a vial containing 10 μL of perchloric acid (4.0 M). The acidified mixtures were vortexed, transferred to ice, centrifuged (16000g, 10 min), and aliquots of the supernatants were subjected to HPLC analysis. The eluent consisted of methanol in phosphate buffer (50 mM, pH 3). The signal detection was carried out as described above. The results reflect a minimum of two replicate determinations. It was demonstrated that a concentration of 2.0 mM for the bicyclic alcohols was saturating by determining the velocity of the glucuronidation reaction at concentrations of 0.5, 1.0, and 2.0 mM showing that the plateau in the Michaelis–Menten plot (velocity versus substrate concentration) was reached between approximately 0.5 and 1.5 mM depending on the substrate used. Substrate inhibition was not detected. Therefore, the velocities measured at a concentration of 2.0 mM yielded good estimates of the  $V_{max}$  values under the conditions of the assay (unsaturating cosubstrate concentration). Nonlinear kinetic behavior due to enzyme denaturation occurred for UGT2B7 after an incubation time of 140 min and for UGT2B17 after 160 min, as demonstrated by progression curves using scopoletin as well as UDPGlcA at saturating concentrations.

**Inhibition Assays.** The IC<sub>50</sub> values of the substrates **1–10** were determined at concentrations of 10, 25, 50, 100, 250, 500, and 1000 μM, and the IC<sub>50</sub> values for the enantiomers of compounds **11–14** were determined at 5, 10, 25, 50, and 100 μM. Scopoletin was employed at 500 μM for UGT2B7 and 300 μM for UGT2B17, and it resembled its  $K_m$  for the respective enzyme (531 and 309 μM, respectively). The  $K_m$  values of scopoletin for UGT2B7 and UGT2B17 were determined frequently in our laboratory, and the values represent the average values of experiments conducted during the last year using the same enzyme batches. The reaction mixture consisted of 5.0 mM phosphate buffer (pH 7.4), 10 mM MgCl<sub>2</sub>, and 5.0 mM saccharic acid-1,4-lactone. The enzymes were employed at 0.1 μg/μL. One control assay in the absence of inhibitor and one blank run in the absence of cosubstrate were included in each inhibition assay. The enzyme reaction was initiated after a 5 min preincubation time (37 °C) by the addition of a solution of UDPGlcA to a final concentration of 5.0 mM. The enzyme reactions were terminated after an incubation time of 15 min at 37 °C by the

addition of perchloric acid (4.0 M), and the mixtures were transferred to ice. The mixtures were centrifuged (16000g, 10 min), and aliquots of the supernatants were subjected to HPLC analysis. The eluent consisted of methanol in phosphate buffer (50 mM, pH 3). Fluorescence excitation and emission wavelengths of 335 and 455 nm, respectively, were optimal for the detection of scopoletin glucuronide. The quantification was carried out by recording standard curves with dilutions of scopoletin glucuronide, which was previously synthesized in our laboratory. The data were analyzed by nonlinear regression applying the two-parameter Hill equation (concentration–response curve). The  $K_{ic}$  values and the mechanism of inhibition for the racemates of compounds **5**, **7**, and **10** were determined by measuring the initial velocities for scopoletin glucuronidation. Scopoletin was used at 100, 250, 500, 1000, and 2000 μM for both UGT isoforms. The enantiomers were applied at three concentrations bracketing their estimated  $K_{ic}$  values, which were calculated by the Cheng–Prusoff equation for competitive inhibition from their respective IC<sub>50</sub> values.<sup>39</sup> The assays were conducted similarly to the determination of IC<sub>50</sub> values. The results reflect a minimum of three replicate determinations.

**Acknowledgment.** This work was supported by a fellowship from the Finnish Cultural Foundation (I.B.) and the Academy of Finland (Project 207535).

**Supporting Information Available:** Degree of purity (elemental analysis), spectroscopic data, statistical data for Tables 2 and 3, results of the inhibition-model selection, and equations. This material is available free of charge via the Internet at <http://pubs.acs.org>.

## References

- Parascandola, J. The Evolution of Stereochemical Concepts in Pharmacology. In *van't Hoff–LeBell Centennial*; Ramsay, O. B., Ed.; American Chemical Society: Washington, DC, 1975; pp 143–158.
- Crossley, R. *Chirality and the Biological Activity of Drugs*; CRC Press: Boca Raton, FL, 1995; 196 pp.
- Eichelbaum, M.; Testa, B.; Somogyi, A. *Stereochemical Aspects of Drug Action and Disposition*; Springer-Verlag: Berlin, 2003; 442 pp.
- Federsel, H. J. Asymmetry on large scale: the roadmap to stereo-selective processes. *Nat. Rev. Drug Discovery* **2005**, *4*, 685–697.
- Ariëns, E. J. Stereochemistry, a basis for sophisticated nonsense in pharmacokinetics and clinical pharmacology. *Eur. J. Clin. Pharmacol.* **1984**, *26*, 663–668.
- Agranat, I.; Caner, H.; Caldwell, A. Putting chirality to work: the strategy of chiral switches. *Nat. Rev. Drug Discovery* **2002**, *1*, 753–768.
- Caldwell, J. Do single enantiomers have something special to offer?. *Hum. Psychopharmacol.* **2001**, *16*, S67–S71.
- Handley, D. A. The therapeutic advantages achieved through single-isomer drugs. *Pharm. News* **1999**, *6*, 11–15.
- Fisher, M. B.; Paine, M. F.; Strelevitz, T. J.; Wrighton, S. A. The role of hepatic and extrahepatic UDP-glucuronosyltransferases in human drug metabolism. *Drug Metab. Rev.* **2001**, *33*, 273–297.
- Inman, W. H.; Rawson, N. S. Zomepirac and cardiovascular deaths. *Lancet* **1983**, *2*, 908.
- Kilpatrick, G. J.; Smith, T. W. Morphine-6-glucuronide: actions and mechanisms. *Med. Res. Rev.* **2005**, *25*, 521–544.
- Wells, P. G.; Mackenzie, P. I.; Chowdhury, J. R.; Guillemette, C.; Gregory, P. A.; Ishii, Y.; Hansen, A. J.; Kessler, F. K.; Kim, P. M.; Chowdhury, N. R.; Ritter, J. K. Glucuronidation and the UDP-glucuronosyltransferases in health and disease. *Drug Metab. Dispos.* **2004**, *32*, 281–290.
- King, C. D.; Rios, G. R.; Green, M. D.; Tephly, T. R. UDP-glucuronosyltransferases. *Curr. Drug Metab.* **2000**, *1*, 143–161.
- Ritter, J. K.; Chen, F.; Sheen, Y. Y.; Tran, H. M.; Kimura, S.; Yeatman, M. T.; Owens, I. S. A novel complex locus UGT1 encodes human bilirubin, phenol, and other UDP-glucuronosyltransferase isozymes with identical carboxyl termini. *J. Biol. Chem.* **1992**, *267*, 3257–3261.
- Monaghan, G.; Clarke, D. J.; Povey, S.; See, C. G.; Boxer, M.; Burchell, B. Isolation of a human YAC contig encompassing a cluster of UGT2 genes and its regional localization to chromosome 4q13. *Genomics* **1994**, *23*, 496–499.

- (16) The carboxyl-terminal portions of UGT1A isoforms are identical due to exon sharing during transcription and RNA processing. In contrast, the human UGT2B proteins are encoded by individual genes on chromosome 4, but the C-terminal halves of the different UGT2B isoforms display high sequence similarities.
- (17) Luukkanen, L.; Taskinen, J.; Kurkela, M.; Kostianen, R.; Hirvonen, J.; Finel, M. Kinetic characterization of the 1A subfamily of recombinant human UDP-glucuronosyltransferases. *Drug Metab. Dispos.* **2005**, *33*, 1017–1026.
- (18) Meech, R.; Mackenzie, P. I. Structure and function of uridine diphosphate glucuronosyltransferases. *Clin. Exp. Pharmacol. Physiol.* **1997**, *24*, 907–915.
- (19) Sorich, M. J.; Miners, J. O.; McKinnon, R. A.; Smith, P. A. Multiple pharmacophores for the investigation of human UDP-glucuronosyltransferase isoform substrate selectivity. *Mol. Pharmacol.* **2004**, *65*, 301–308.
- (20) Sorich, M. J.; McKinnon, R. A.; Miners, J. O.; Winkler, D. A.; Smith, P. A. Rapid prediction of chemical metabolism by human UDP-glucuronosyltransferase isoforms using quantum chemical descriptors derived with the electronegativity equalization method. *J. Med. Chem.* **2004**, *47*, 5311–5317.
- (21) Turgeon, D.; Carrier, J. S.; Levesque, E.; Hum, D. W.; Belanger, A. Relative enzymatic activity, protein stability, and tissue distribution of human steroid-metabolizing UGT2B subfamily members. *Endocrinology* **2001**, *142*, 778–787.
- (22) Turgeon, D.; Carrier, J. S.; Chouinard, S.; Belanger, A. Glucuronidation activity of the UGT2B17 enzyme toward xenobiotics. *Drug Metab. Dispos.* **2003**, *31*, 670–676.
- (23) Court, M. H.; Duan, S. X.; Guillemette, C.; Journault, K.; Krishnaswamy, S.; von Moltke, L. L.; Greenblatt, D. J. Stereoselective conjugation of oxazepam by human UDP-glucuronosyltransferases (UGTs): *S*-oxazepam is glucuronidated by UGT2B15, while *R*-oxazepam is glucuronidated by UGT2B7 and UGT1A9. *Drug Metab. Dispos.* **2002**, *30*, 1257–1265.
- (24) Bichlmaier, I.; Siiskonen, A.; Finel, M.; Yli-Kauhaluoma, J. Chiral distinction between the enantiomers of bicyclic alcohols by UDP-glucuronosyltransferases 2B7 and 2B17. *Biol. Chem.*, in press.
- (25) Gentili, F.; Bousquet, O.; Brasili, L.; Dontenwill, M.; Feldman, J.; Ghelfi, F.; Giannella, M.; Piergentili, A.; Quaglia, W.; Pignini, M. Imidazole binding sites (IBS) profile modulation: key role of the bridge in determining I1-IBS or I2-IBS selectivity within a series of 2-phenoxymethylimidazole analogues. *J. Med. Chem.* **2003**, *46*, 2169–2176.
- (26) Johansen, T. N.; Stensbol, T. B.; Nielsen, B.; Vogensen, S. B.; Frydenvang, K.; Slok, F. A.; Brauner-Osborne, H.; Madsen, U.; Krosgaard-Larsen, P. Resolution, configurational assignment, and enantiopharmacology at glutamate receptors of 2-amino-3-(3-carboxy-5-methyl-4-isoxazolyl)propionic acid (ACPA) and demethyl-ACPA. *Chirality* **2001**, *13*, 523–532.
- (27) Bogeso, K. P.; Arnt, J.; Hyttel, J.; Pedersen, H. Stereospecific and selective 5-HT<sub>2</sub> antagonism in a series of 5-substituted *trans*-1-piperazino-3-phenylindans. *J. Med. Chem.* **1993**, *36*, 2761–2770.
- (28) Corey, E. J.; Bakshi, R. K.; Shibata, S. Highly enantioselective borane reduction of ketones catalyzed by chiral oxazaborolidines. Mechanism and synthetic implications. *J. Am. Chem. Soc.* **1987**, *109*, 5551–5553.
- (29) Corey, E. J.; Helal, C. J. Reduction of carbonyl compounds with chiral oxazaborolidine catalysts: a new paradigm for enantioselective catalysis and a powerful new synthetic method. *Angew. Chem., Int. Ed.* **1998**, *37*, 1986–2012.
- (30) Garrett, C. E.; Prasad, K.; Repic, O.; Blacklock, T. J. The enantioselective reduction of 2'-fluoroacetophenone utilizing a simplified CBS-reduction procedure. *Tetrahedron: Asymmetry* **2002**, *13*, 1347–1349.
- (31) Xu, J.; Wei, T.; Zhang, Q. Influences of electronic effects and anions on the enantioselectivity in the oxazaborolidine-catalyzed asymmetric borane reduction of ketones. *J. Org. Chem.* **2004**, *69*, 6860–6866.
- (32) Salunkhe, A. M.; Burkhardt, E. R. Highly enantioselective reduction of prochiral ketones with *N,N*-diethylaniline borane (DEANB) in oxazaborolidine-catalyzed reductions. *Tetrahedron Lett.* **1997**, *38*, 1523–1526.
- (33) Barlow, R. B.; Franks, F. M.; Pearson, J. D. M. Relation between biological activity and degree of resolution of optical isomers. *J. Pharm. Pharmacol.* **1972**, *24*, 753–761.
- (34) The authors prefer the term “diastereoselective glucuronidation” over “enantioselective glucuronidation,” although the latter is often encountered in the literature. However, the products of the UGT-catalyzed glucuronidation, the glucuronide of the (*R*)-enantiomer and the glucuronide of its respective (*S*)-enantiomer, are related as diastereomers. Therefore, the UGT-catalyzed conjugation is diastereoselective provided that the formation of one of the two diastereomers is favored (Moss, G. P. Basic Terminology of Stereochemistry (IUPAC Recommendations 1996). *Pure Appl. Chem.* **1996**, *68*, 2193–2222). This preferential formation of one diastereomer over the other is also termed substrate–product stereoselectivity or substrate–product stereospecificity.
- (35) The authors are aware of the fact that the cosubstrate concentration of 120 μM is below the physiological concentration of UDPGlcA and below the enzymes' *K<sub>m</sub>* for this cosubstrate. However, this concentration was sufficient to investigate the stereoselectivity with respect to the GlcA-transfer reaction. The cosubstrate concentration was limited due to the high costs of radiolabeled [<sup>14</sup>C]UDPGlcA as well as to minimize the radioactive waste output.
- (36) Kaivosari, S.; Salonen, J. S.; Mortensen, J.; Taskinen, J. High-performance liquid chromatographic method combining radiochemical and ultraviolet detection for determination of low activities of uridine 5'-diphosphate-glucuronosyltransferase. *Anal. Biochem.* **2001**, *292*, 178–187.
- (37) Agranat, I.; Sarel, S. Reflections on chiral discrimination. Discrimination is between equals, distinction is between unequals. *Enantiomer* **1996**, *1*, 249–250.
- (38) Pfeiffer, C. C. Optical isomerism and pharmacological action, a generalization. *Science* **1956**, *124*, 29–31.
- (39) Cheng, Y.; Prusoff, W. H. Relationship between the inhibition constant (*K<sub>i</sub>*) and the concentration of inhibitor which causes 50% inhibition (*I<sub>50</sub>*) of an enzymatic reaction. *Biochem. Pharmacol.* **1973**, *22*, 3099–3108.
- (40) The maximum inhibition attained by the enantiomers of the lipophilic alcohols **11–13** ranged merely between 9.1% and 55%, even though the scopoletin concentration was lowered to 50 μM. However, the enantiomers of each compound showed similar inhibition levels at the highest concentration of 0.10 mM. Therefore, the enantiomers of these lipophilic compounds exerted similar affinities to the enzymes (cf. Supporting Information).
- (41) Kurkela, M.; Garcia-Horsman, J. A.; Luukkanen, L.; Mörsky, S.; Taskinen, J.; Baumann, M.; Kostianen, R.; Hirvonen, J.; Finel, M. Expression and characterization of recombinant human UDP-glucuronosyltransferases (UGTs). UGT1A9 is more resistant to detergent inhibition than other UGTs and was purified as an active dimeric enzyme. *J. Biol. Chem.* **2003**, *278*, 3536–3544.